ISSN NO. 2320-5407

Journal homepage: http://www.journalijar.com

INTERNATIONAL JOURNAL OF ADVANCED RESEARCH

RESEARCH ARTICLE

Benzamide, acetamide and acrylamide as Corrosion Inhibitors for Carbon Steel in Hydrochloric Acid Solutions

*** A.S.Fouda[1], A.M.Eldesoky [2], M.A.Elmorsi [3], M.Y.El sheik [3]and I.A.El said[3]**

1.Department of Chemistry, Faculty of Science, El-Mansoura University, El-Mansoura-35516, Egypt:

2. Engineering Chemistry Department, High Institute of Engineering &Technolog(New Damietta), Egypt and Chemistry Department, Qunfudah University College, Umm Al-Qura University, KSA

3.Department of Chemistry, Faculty of Science, Tanta University, Egypt

Manuscript Info

Manuscript History:

Received: 12 December 2013
Final Accepted: 29 January 2014
Published Online: February 2014

Key words:
Corrosion inhibition, amide compounds, HCl, EIS, SEM, EDX**.**

****Corresponding Author***

A.S.Fouda

Abstract

The corrosion inhibition characteristics of some amide compounds, namely benzamide, acetamide and acrylamide on the carbon steel corrosion in 1 M hydrochloric acid have been investigated at 30°C by weight loss, potentiodynamic polarization, electrochemical frequency modulation (EFM) and electrochemical impedance spectroscopy (EIS) techniques. The inhibition efficiencies obtained from all methods employed are in good agreement with each other. The obtained results show that benzamide is the best inhibitor with an efficiency of 90.9% at 5 x 10^{-3} M additive concentration. Generally, the inhibition efficiency increased with increasing the inhibitor concentration. Changes in impedance parameters (charge transfer resistance, R_{ct}, and double-layer capacitance, C_{dl}) were indicative of adsorption of benzamide on the metal surface, leading to the formation of a protective film. The potentiodynamic polarization measurements indicated that the inhibitors are of mixed type. The adsorption of the inhibitors on the carbon steel surface in the acid solution was found to obey Temkin's adsorption isotherm. The free energies of adsorption were calculated and discussed. The surface morphology of inhibited carbon steel was analyzed by scanning electron microscope (SEM) and with energy dispersive X-ray spectroscopy (EDX).

Copy Right, IJAR, 2014,. All rights reserved.

Introduction

Carbon steel has been extensively used under different conditions in petroleum industries [1]. Aqueous solutions of acids are among the most corrosive media. Acid solutions are widely used in industries for pickling, acid cleaning of boilers, descaling and oil well acidizing [2–5]. Mostly, sulfuric and hydrochloric acids are employed for such purposes [6]. The main problem concerning carbon steel applications is its relatively low corrosion resistance in acidic solutions. Several methods are currently used to prevent corrosion of carbon steel. One such method is the use of an organic inhibitor [7,8]. Effective inhibitors are heterocyclic compounds that have bonds, heteroatom phosphorus, sulfur, oxygen and nitrogen [9,10]. The compounds containing both nitrogen and sulfur can provide excellent inhibition, compared with compounds containing only nitrogen or sulfur [11]. Heterocyclic compounds, such as mercapto-triazole [12] and 2-mercapto-1-methylimidazol have been used to inhibit mild steel corrosion in acidic solutions. The efficiency of an inhibitor is largely dependent on its adsorption on the metal surface, which consists of replacement of water molecules by the organic inhibitor at the interface [13]. The adsorption of these molecules depends mainly on certain physicochemical properties of the inhibitor molecule such as functional groups, steric factors, aromaticity, electron density at the donor atoms and orbital character of donating electrons and the electronic structure of the molecules [14]. Regarding the adsorption of inhibitor on the metal surface, two types of interactions are responsible. One is physical adsorption, which involves electrostatic forces between ionic charges or dipoles of the adsorbed species and the electric charge at metal/solution interface. The other is chemical adsorption,

which involves charge sharing or charge transfer from inhibitor molecules to the metal surface to form coordinate types of bond [15-18]. The selection of appropriate inhibitors mainly depends on the type of acid, its concentration, temperature, the presence of dissolved inorganic and/or organic substances even in minor amounts and, of course, on the type of metallic material supposed to be protected

This work is devoted to study the corrosion inhibition of some amide compounds on the carbon steel in HCl solutions and to determine thermodynamic activation and adsorption parameters of amide compounds .Also, to examine the carbon steel surface by scanning electron microscopy (SEM) and energy dispersed before and after exposing it to the corrosive medium.

2. Experimental methods

2.1. Materials

Materials used for the study were carbon steel sheet of composition (weight %) 0.200 C, 0.003 Si, 0.024 P, 0.350 Mn, the rest Fe.

2.2. Chemicals and solutions

2.2.1. Chemicals

Hydrochloric acid (BDH grade) and amide compounds (BDH grade) were purchased from Aldrich-Sigma Company. The inhibitors used in this study were listed in Table (1):

Table (1): Molecular structures, names, molecular weights and molecular formulas of investigated amide compounds

Compound No.	Structures	Names	Mol. Weights and Mol. Formulas
1	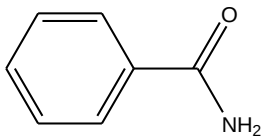	benzamide	C_7H_7NO 121.14
2	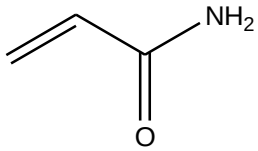	acetamide	C_3H_5NO 71.08
3	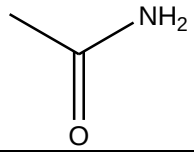	acrylamide	C_2H_5NO 59.07

2.3. Weight loss method

Carbon steel sheets of 20 x 20 x 2 mm were abraded with different grades of emery paper up to 1200 grit and then washed with bidistilled water and acetone. After weighing accurately, the specimens were immersed in 100 ml HCl solution with and without addition of different concentrations of inhibitors. After 3 hrs, the specimens were taken out, washed, dried, and weighed accurately. The average weight loss of the three parallel carbon steel sheets could be obtained at required temperature. The inhibition efficiency (% IE) and the degree of surface coverage (θ) of the investigated inhibitors on the corrosion of carbon steel were calculated as follows [19]:

$$\% IE = \theta \times 100 = [(W_o - W)/ W_o] \times 100 \quad (1)$$

where W_o and W are the values of the average weight losses in the absence and presence of the inhibitor, respectively.

2.4. Electrochemical measurements

The experiments were carried out potentiodynamically in a thermostated three electrode cell. Platinum foil was used as counter electrode (1 cm^2) and a saturated calomel electrode (SCE) coupled to a fine Luggin capillary as the reference electrode. The working electrode was in the form of a square cut from carbon steel under investigation and was embedded in a Teflon rod with an exposed area of 1 cm^2. This electrode was immersed in 100 ml of a test solution for 30 min until a steady state open-circuit potential (Eocp) was attained. The potentiodynamic curves were recorded by changing the electrode potential from -1.0 to 0.0 V versus SCE with scan rate of 5 mVs^{-1}. All experiments were carried out in freshly prepared solution at constant temperature (30 $\pm 1^oC$) using a thermostat. %IE and the degree of surface coverage (θ) were defined as:

$$\%IE = \theta \times 100 = [(i_{corr} - i_{corr(inh)}) / i_{corr}] \times 100 \quad (2)$$

where i_{corr} and $i_{corr(inh)}$ are the uninhibited and inhibited corrosion current density values, respectively, determined by extrapolation of Tafel lines.

The electrochemical impedance spectroscopy (EIS) spectra were recorded at open circuit potential (OCP) after immersion the electrode for 30 min in the test solution. The ac signal was 5 mV peak to peak and the frequency range studied was between 100 kHz and 0.2 Hz.

The inhibition efficiency (% IE) and the surface coverage (θ) of the used inhibitors obtained from the impedance measurements were calculated by applying the following relations:

$$\% IE = \theta \times 100 = [1-(R^{\circ}_{ct}/R_{ct})] \quad (3)$$

where, R^o_{ct} and R_{ct} are the charge transfer resistance in the absence and presence of inhibitor, respectively.

EFM experiments were performed with applying potential perturbation signal with amplitude 10 mV with two sine waves of 2 and 5 Hz. The choice for the frequencies of 2 and 5Hz was based on three arguments [20]. The larger peaks were used to calculate the corrosion current density (i_{corr}), the Tafel slopes (β_c and β_a) and the causality factors CF-2 and CF-3 [21].

All electrochemical experiments were carried out using Gamry instrument PCI300/4 Potentiostat/Galvanostat/Zra analyzer, DC105 Corrosion software, EIS300 Electrochemical Impedance Spectroscopy software, EFM140 Electrochemical Frequency Modulation software and Echem Analyst 5.5 for results plotting, graphing, data fitting and calculating.

2.5 SEM-EDX Measurement

The carbon steel surface was prepared by keeping the specimens for 3 days immersion in 1 M HCl in the presence and absence of optimum concentrations of amide compounds, after abraded using different emery papers up to 1200 grit size. Then, after this immersion time, the specimens were washed gently with distilled water, carefully dried and mounted into the spectrometer without any further treatment. The corroded carbon steel surfaces were examined using an X-ray diffractometer Philips (pw-1390) with Cu-tube (Cu Ka1, l = 1.54051 A°), a scanning electron microscope (SEM, JOEL, JSM-T20, Japan).

2. 6. Theoretical study

Accelrys (Material Studio Version 4.4) software for quantum chemical calculations has been used.

3. Results and discussion

3.1. Weight loss measurements

Figure (1) represents the weight loss-time curves in the absence and presence of different concentrations of compound (1). Similar curves were obtained for other inhibitors (not shown). Table (2) collects the values of inhibition efficiency obtained from weight loss measurements in 1 M HCl at 30°C. The results of this Table show that the presence of inhibitors reduces the corrosion rate of carbon steel in 1 M HCl and hence, increase the inhibition efficiency. The inhibition achieved by these compounds decreases in the following order: Compound (1) > Compound (2) > Compound (3)

Figure (1): Weight loss-time curves for the dissolution of C-steel in 1M HCl in the absence and presence of different concentrations of compound (1) at 30°C

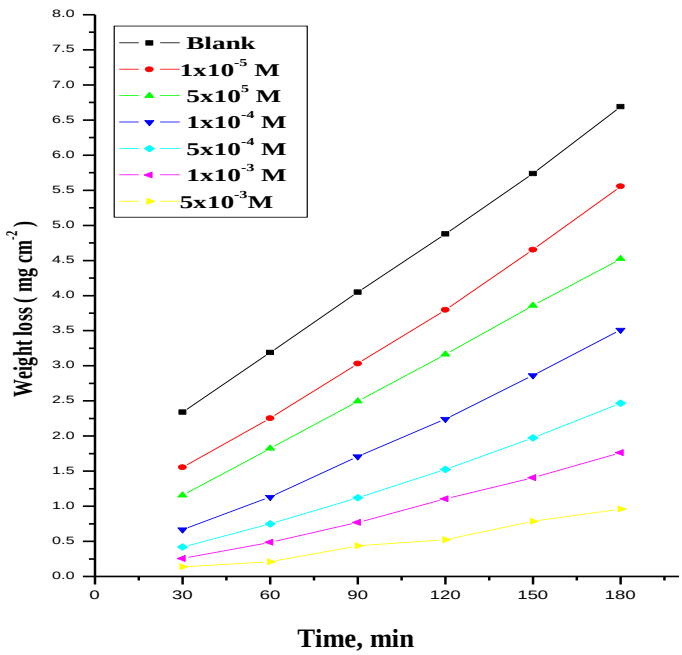

Table (2): Inhibition efficiency of all inhibitors at different concentrations of inhibitors as determined from weight loss method for carbon steel at 30°C

Conc., M	% IE		
	(1)	(2)	(3)
$1x10^{-6}$	38.6	30.1	26.9
$5x10^{-6}$	73.9	45.5	30.4
$1x10^{-4}$	80.8	75.5	72.7
$5x10^{-4}$	80.9	80.6	78.1
$1x10^{-3}$	88.4	83.8	78.8
$5x10^{-3}$	90.9	89.6	84.3

3.1.1. Adsorption isotherm

Basic information on the interaction between the inhibitor and the metal surface can be provided by the adsorption isotherm, and the type of the inhibitors on metal is influenced by (i) the nature and charge of the metal (ii) chemical structure of the inhibitor and (iii) the type of electrolyte.

The values of (θ) for different concentrations of the studied compounds at 30°C have been used to explain the best isotherm to determine the adsorption process. The adsorption of the organic derivatives, on the surface of carbon steel electrode may regarded as a substitution adsorption process between organic compounds in aqueous phase (org_{aq}) and the water molecules adsorbed on carbon steel surface (H_2O_{ads}) [22]:

$Org_{(sol)} + x\,(H_2O)_{ads} \leftrightarrow Org_{(ads)} + x\,H_2O_{(sol)}$ (4)

where x is the number of water molecules replaced by one organic molecule. Attempts were made to fit (θ) values to various isotherms, including Langmuir [23], Frumkin [24], and Temkin isotherms [25,26]. In this study, Temkin adsorption isotherm was found to be most suitable for the experimental findings. This isotherm is described by equation (5) with 0.954 – 0.991 regression coefficients as depicted from Figure (2).

$2a\Theta = \ln (K_{ads}\, C)$ (5)

where C is the inhibitor concentration, K_{ads} is the adsorption equilibrium constant and a is heterogeneous factor of metal surface. Equilibrium constant (K_{ads}.) of adsorption process determined using (6) could be further used to determine free energy of adsorption (ΔG^o_{ads}) as follows:

$\Delta G^o_{ads} = - RT \ln (55.5\, K_{ads})$ (6)

where 55.5 is the concentration of water in the solution in mol/L. On the other hand, it is found that the kinetic-thermodynamic model of El-Awady et al [27]:

$\log (\theta / (1-\theta)) = \log K' + y \log C$ (7)

Is valid to operate the present adsorption data. The equilibrium constant of adsorption $K_{ads} = K'\,(1/y)$, where 1/y is the number of the surface active sites occupied by one inhibitors molecule and C is the bulk concentration of the inhibitor. The calculated values of 1/y, K_{ads} and ΔG°_{ads} are given in Table (3). It is worth noting that the value of 1/y is more than unity. This means that the given inhibitor molecules will occupy more than one active site. In general, the values of ΔG°_{ads} were obtained from El-Awady et al model are comparable with those obtained from Temkin's isotherm. From these results it may be generalized that the more efficient inhibitor has more negative ΔG°_{ads} value so that from the tabulated values of ΔG°_{ads} the order of inhibition efficiency is as follows: compound (1) > compound (2) > compound (3). Values of K_{ads} and ΔG^o_{ads} for amide compounds were calculated and are recorded in Table (3). The negative value of "a" indicates the presence of repulsive force between the adsorbed species of amide compounds while the high negative values of ΔG^o_{ads} indicate that these derivatives are strongly adsorbed (chemisorption) on carbon steel surface. The negative value ensures that spontaneity of the adsorption process and the stability of adsorbed layer on the carbon steel surface. The values of K_{ads} were found to run parallel to the % IE [K (1) > K (2) > K (3)]. This result reflects the increasing capability, due to structural formation, on the metal surface [28].

Figure (2): Temkin adsorption isotherm plotted as θ vs. log C of the investigated inhibitors for corrosion of carbon steel in 1 M HCl solution from weight loss method at 30°C

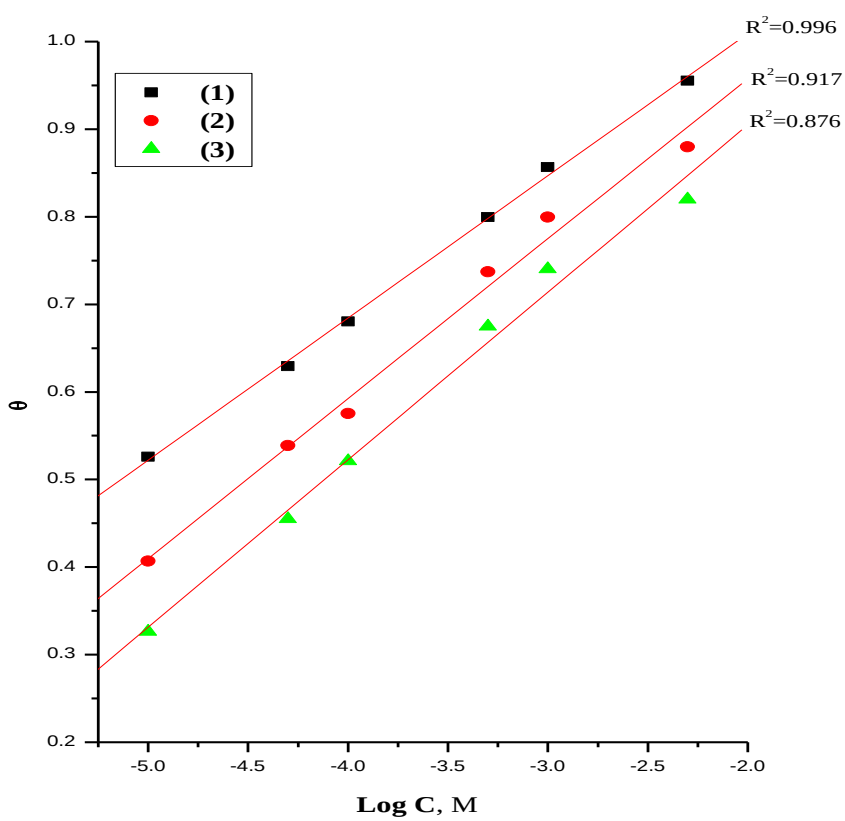

Figure (3): Kinetic-thermodynamic model plotted as log (θ/1- θ) vs. log C of the investigated inhibitors for corrosion of carbon steel in 1 M HCl solution from weight loss method at 30°C

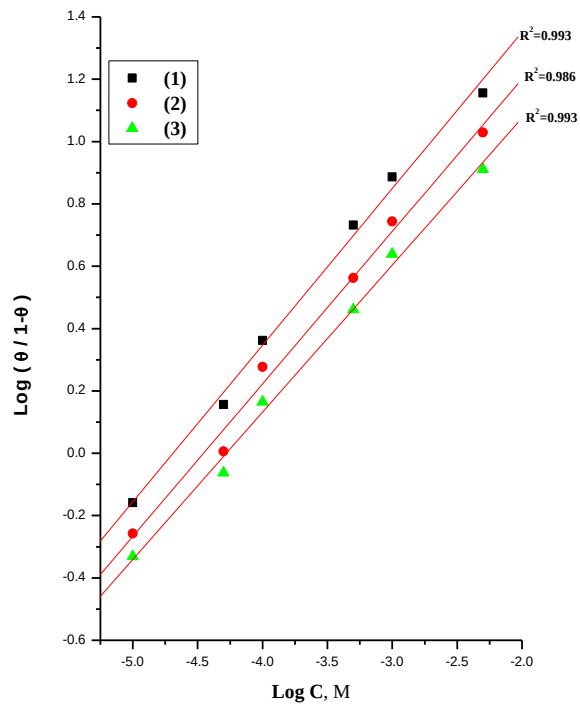

Table (3): Inhibitor binding constant (K_{ads}), free energy of binding ($\Delta G°_{ads}$.), number of active sites (1/y) and later interaction parameter (a) for inhibitors derivatives at 30°C

Inhibitor	Kinetic model			Temkin		
	1 / y	K_{ads} x 10^{-5} M^{-1}	$-\Delta G°_{ads}$ kJ mol^{-1}	a	K_{ads} x 10^{-5} M^{-1}	$-\Delta G°_{ads}$ kJ mol^{-1}
(1)	1.98	46.2	37.3	13.6	217.4	58.5
(2)	2.04	27.9	35.9	10.0	33.2	47.9
(3)	2.11	19.0	34.9	9.8	19.7	46.6

3.1.2. Effect of temperature

To investigate the mechanism of inhibition and to determine the activation energy of corrosion process, weight loss of carbon steel in 1M HCl were studied at various temperatures (30–60°C) in the absence and presence of different concentrations of amide compounds. These inhibitors retard the corrosion process at lower temperatures [29] whereas the inhibition is considerably decreased at elevated temperatures. The increasing of the corrosion rate with increasing the temperature is suggestive of physical adsorption of the investigated inhibitors on carbon steel surface. Fig.(4) represents the Arrhenius plots of natural logarithm of corrosion rate versus 1/T, for carbon steel in 1 M HCl solution, in absent and presence of different concentration of inhibitor (1). The values of slopes of these straight lines permit the calculation of the activation energy, E_a^*, according to:

$$k = A \exp(-E_a^* / RT) \quad (8)$$

where k is the corrosion rate, A is the pre-exponential factor, E_a^* is the apparent activation energy, R is the universal gas constant and T is the absolute temperature.

The values of E_a^* are given in Table (4). The results of Table (4) revealed that, the values of E_a^* were increased by increasing the concentration of the investigated inhibitors indicating the dissolution of carbon steel under these conditions is activation controlled and also, indicates the energy barrier of the corrosion reaction increases in the presence of these additives. Similar results were obtained by other authors [30-32]. The higher values of E_a^* are good evidence for the strong adsorption of compound (1) on carbon steel surface. Also, free energy of activation (ΔG^*) were calculated by applying the transition state equation [33]:

$$\Delta G^* = RT\,[\ln(kT/h) - \ln(\text{corrosion rate})] \quad (9)$$

where, h is Planck's constant and k is Boltzmann's constant. The enthalpy of activation (ΔH^*) and the entropy of activation (ΔS^*) were calculated by applying the following equations [34]:

$$\Delta H^* = E_a^* - RT \quad (10)$$

$$\Delta S^* = (\Delta H^* - \Delta G^*)/T \quad (11)$$

The values of (ΔH^*) are positive and higher in the presence of the inhibitors than in its absence. This implies that energy barrier of the corrosion reaction in the presence of the investigated compounds increases and indicates the endothermic behavior of the corrosion process. On the other hand ΔS^* values are lower and have negative values in presence of the additives, this means that addition of these compounds cause a decrease in the disordering in going from reactants to the activated complexes [35, 36].

Figure (4): Arrhenius plots (log k vs 1/T) for carbon steel in 1M HCl in absence and presence of different concentrations of compound (1)

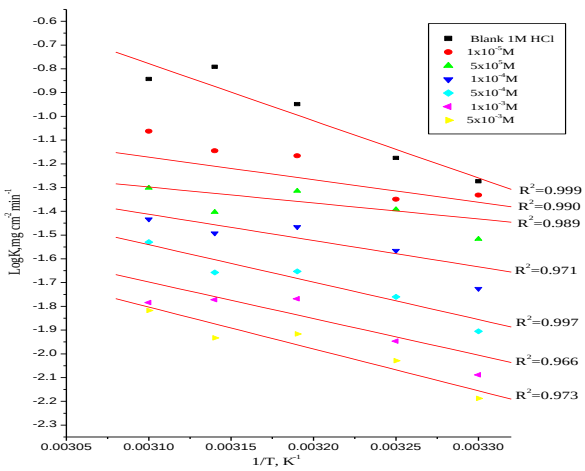

Figure (5): Plots of (log k /T vs 1/T) for corrosion of carbon steel in 1M HCl in absence and presence of different concentrations of compound (1)

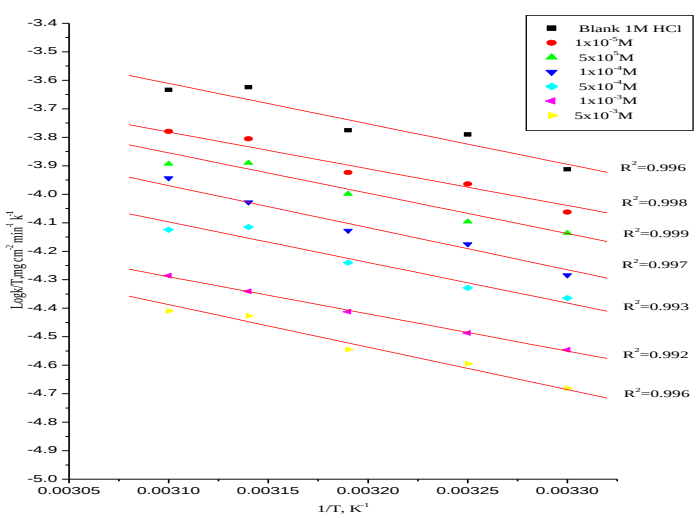

Table (4): Activation parameters for the dissolution of carbon steel in presence and absence of different concentrations of inhibitors in 1M HCl

Inhibitor	Conc., M	Activation parameters		
		E_a^*	ΔH^*	$-\Delta S^*$
		kJ mol^{-1}	kJ mol^{-1}	J mol^{-1} K^{-1}
Free Acid 1M HCl)(	0.0	14.8	21.9	178.1
Compound (1)	1 x 10^{-5}	68.8	49.5	174.4
	5 x 10^{-5}	68.9	50.3	174.0
	1 x 10^{-4}	69.1	52.9	173.8
	5 x 10^{-4}	69.9	55.4	172.3
	1 x 10^{-3}	72.8	5702	168.3
	5 x 10^{-3}	76.6	58.4	166.8
Compound (2)	1 x 10^{-5}	41.1	23.5	174.6
	5 x 10^{-5}	42.5	24.4	174.4
	1 x 10^{-4}	44.5	29.5	159.3
	5 x 10^{-4}	47.7	31.3	155.1
	1 x 10^{-3}	52.0	31.8	154.9
	5 x 10^{-3}	55.5	53.9	87.8
Compound (3)	1 x 10^{-5}	14.9	26.6	70.4
	5 x 10^{-5}	16.1	27.1	68.9
	1 x 10^{-4}	24.0	27.3	68.3
	5 x 10^{-4}	24.9	28.3	68.2
	1 x 10^{-3}	30.2	25.0	67.7
	5 x 10^{-3}	33.6	28.5	64.3

3.2. Potentiodynamic polarization measurements

Figure (6) shows the potentiodynamic polarization curves for carbon steel without and with different concentrations of compound (1) at 30°C. Similar curves were obtained for other compounds (not shown). The obtained electrochemical parameters; cathodic (β_c) and anodic (β_a) Tafel slopes, corrosion potential (E_{corr}), and corrosion current density (i_{corr}), were obtained and listed in Table (5). Table (5) shows that i_{corr} decreases by adding the amide compounds and by increasing their concentration. In addition, E_{corr} does not change obviously. Also β_a and β_c do not change markedly, which indicates that the mechanism of the corrosion reaction of carbon steel does not change. Figure (6) clearly shows that both anodic and cathodic reactions are inhibited, which indicates that investigated compounds act as mixed-type inhibitors [37, 38]. The inhibition achieved by these compounds decreases in the following order: compound (1) > compound (2) > compound (3). The percentage inhibition efficiencies (% IE) calculated from i_{corr} of the investigated compounds is given in Table (5). An inspection of the results obtained from this Table reveals that, the presence of different concentrations of the additives reduces the anodic and cathodic current densities. This indicates the inhibiting effects of the investigated compounds. The order of decreasing inhibition efficiency from i_{corr} is: compound (1) > compound (2) > compound (3).The values of % IE determined from the two methods are very close to each other indicating the validity of the obtained results.

Figure (6): Potentiodynamic polarization curves for the corrosion of carbon steel in 1M HCl in the absence and presence of various concentrations of compound (1) at 30°C

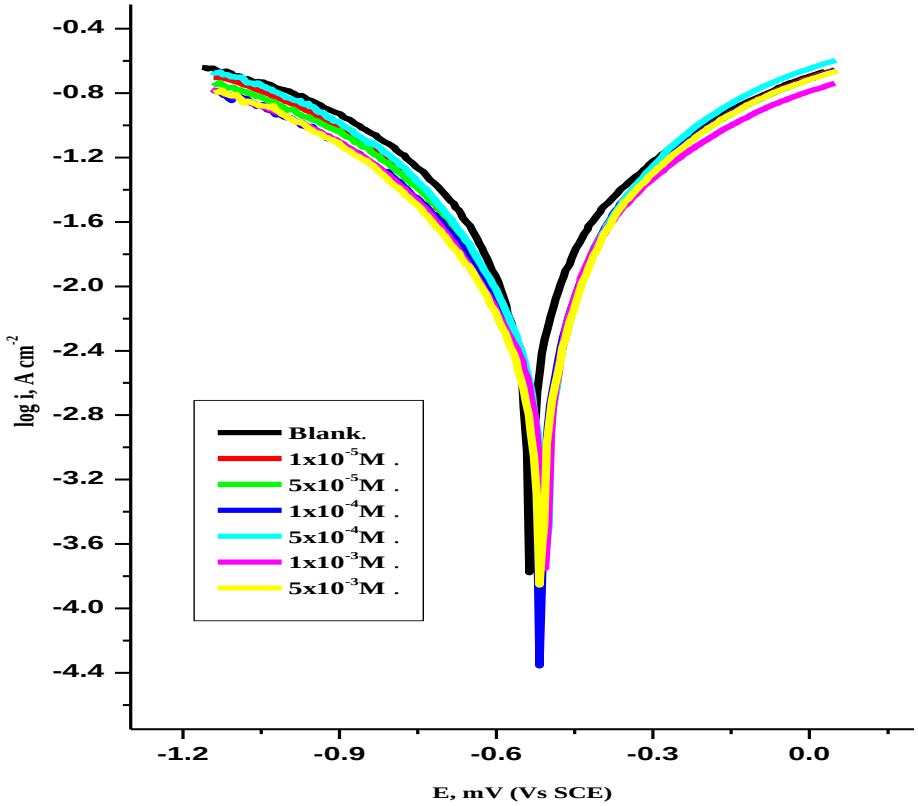

Table (5): Effect of concentrations of the investigated compounds on the free corrosion potential ($E_{corr.}$), corrosion current density ($i_{corr.}$), Tafel slopes (β_a& β_c), degree of surface coverage (θ) and inhibition efficiency (% IE) for carbon steel in 1M HCl at 30°C

Concentration, M		$i_{corr.}$ mA cm^{-2}	$-E_{corr.}$ mV vs.SCE	β_a mV dec^{-1}	β_c mV dec^{-1}	θ	% IE
0.0		956	5.099 x 10^{-4}	438	461	---	----
Compound (1)	1 x 10^{-5}	467	4.870 x 10^{-4}	204	193	0.045	4.5
	5 x 10^{-5}	459	1.942 x 10^{-4}	186	174	0.620	62.0
	1 x 10^{-4}	454	1.674 x 10^{-4}	176	165	0.672	67.2
	5 x 10^{-4}	451	1.266 x 10^{-4}	161	163	0.752	75.2
	1 x 10^{-3}	499	4.321 x 10^{-5}	157	154	0.915	91.5
	5 x 10^{-3}	428	3.680 x 10^{-5}	154	146	0.993	99.3
Compound (2)	1 x 10^{-5}	492	4.878 x 10^{-4}	215	235	0.043	4.3
	5 x 10^{-5}	473	4.304 x 10^{-4}	180	215	0.156	15.6
	1 x 10^{-4}	467	3.296 x 10^{-4}	172	191	0.353	35.3

	5×10^{-4}	454	1.829×10^{-4}	153	179	0.641	64.1
	1×10^{-3}	438	5.646×10^{-5}	151	135	0.889	88.9
	5×10^{-3}	436	4.878×10^{-5}	147	106	0.904	90.4
Compound (3)	1×10^{-5}	475	5.091×10^{-4}	215	241	0.002	0.2
	5×10^{-5}	474	4.884×10^{-4}	212	235	0.042	4.2
	1×10^{-4}	474	3.410×10^{-4}	193	192	0.331	33.1
	5×10^{-4}	473	3.105×10^{-4}	183	169	0.391	39.1
	1×10^{-3}	459	3.045×10^{-4}	180	162	0.403	40.3
	5×10^{-3}	453	5.979×10^{-5}	147	158	0.883	88.3

3.3. Electrochemical Impedance Spectroscopy (EIS)

The corrosion of carbon steel in 1 M HCl in the presence of the investigated compounds was investigated by EIS method at 30°C after 30 min immersion. Nyquist plots in the absence and presence of investigated compound (1) are presented in Figure (7). Similar curves were obtained for other inhibitors (not shown). It is apparent that all Nyquist plots show a single capacitive loop, both in uninhibited and inhibited solutions. The impedance data of carbon steel in 1 M HCl are analyzed in terms of an equivalent circuit model Figure (8) which includes the solution resistance R_s and the double layer capacitance C_{dl} which is placed in parallel to the charge transfer resistance R_{ct} [39] due to the charge transfer reaction. For the Nyquist plots it is obvious that low frequency data are on the right side of the plot and higher frequency data are on the left. This is true for EIS data where impedance usually falls as frequency rises (this is not true for all circuits). The capacity of double layer (C_{dl}) can be calculated from the following equation:

$$C_{dl} = \frac{1}{2} \pi f_{max} R_{ct} \qquad (12)$$

where f_{max} is maximum frequency. The parameters obtained from impedance measurements are given in Table (6). It can see from Table (6) that the values of charge transfer resistance R_{ct} increase with inhibitor concentration [40]. In the case of impedance studies, % IE increases with inhibitor concentration in the presence of investigated inhibitors and the % IE of these investigated inhibitors is as follows: compound (1) > compound (2) > compound (3)

The impedance study confirms the inhibiting characters of these compounds obtained from potentiodynamic polarization and weight loss methods. It is also noted that the (C_{dl}) values tend to decrease when the concentration of these compounds increases. This decrease in (C_{dl}), which can result from a decrease in local dielectric constant and/or an increase in the thickness of the electrical double layer, suggests that these compounds molecules function by adsorption at the metal/solution interface [41]. The inhibiting effect of these compounds can be attributed to their parallel adsorption at the metal solution interface. The parallel adsorption is owing to the presence of one or more active center for adsorption.

Figure (7): The Nyquist (a) and Bode (b) plots for corrosion of carbon steel in 1M HCl in the absence and presence of different concentrations of compound (1) at 30°C

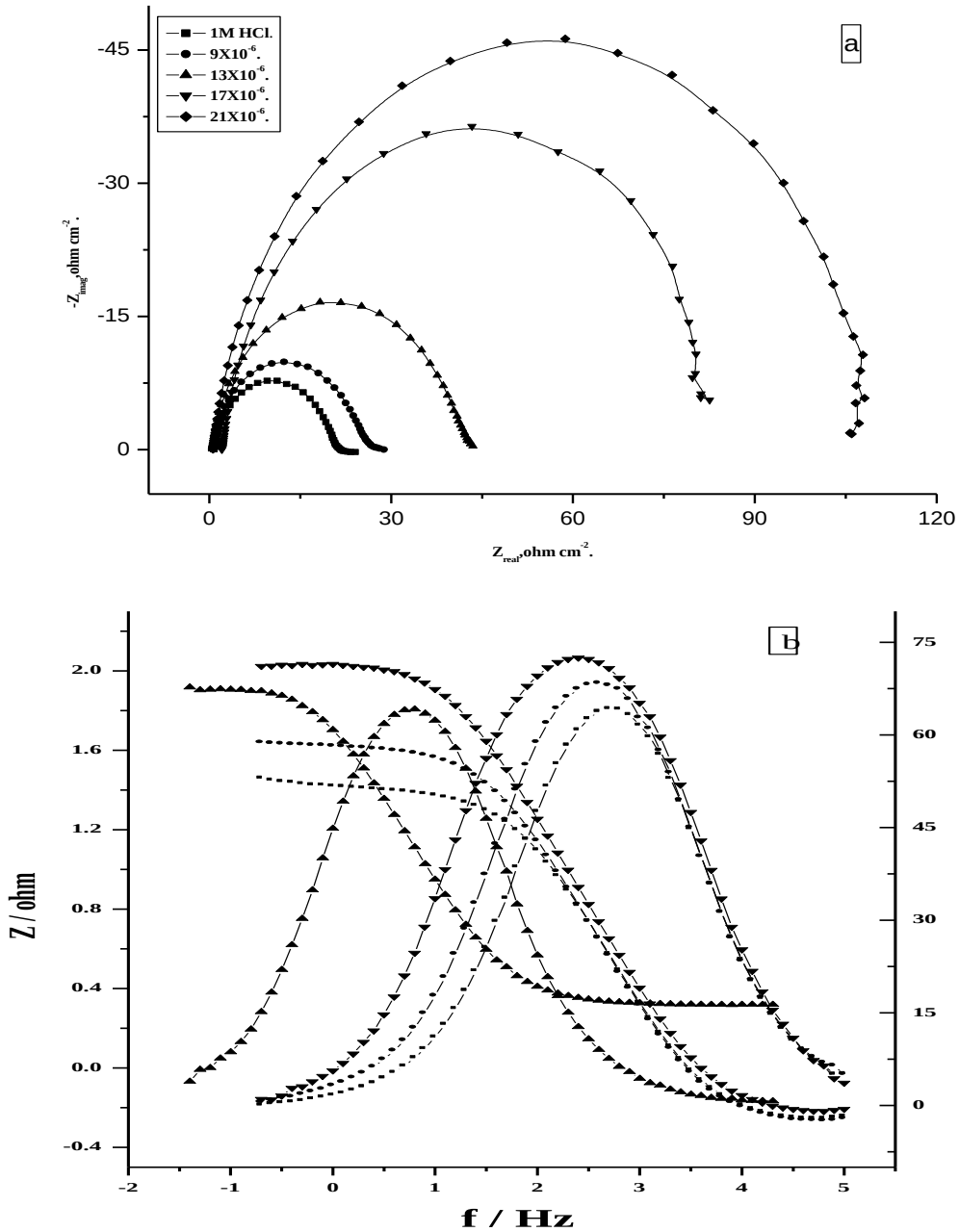

Figure (8): Equivalent circuit model used to fit the impedance spectra

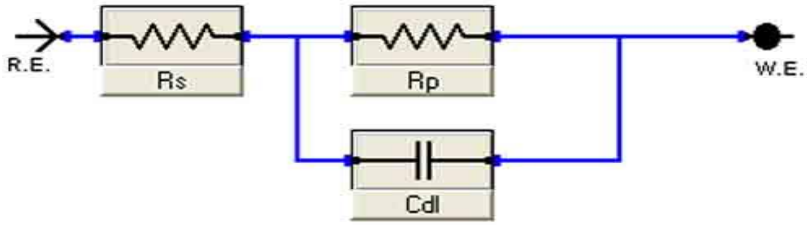

Table (6): Electrochemical kinetic parameters obtained from EIS technique for the corrosion of carbon steel in 1 M HCl at different concentrations of investigated inhibitors at 30°C

compounds	Concentration, M	C_{dl}, μF cm^{-2}	R_{ct}, ohm cm^2	θ	% IE
Blank	1 M HCl	36.8	*27.5*	-	-
Compound (1)	1×10^{-5}	4.1	246.6	0.888	88.8
	5×10^{-5}	3.9	256.3	0.893	89.3
	1×10^{-3}	3.4	302.9	0.909	90.9
	5×10^{-3}	3.1	323.9	0.915	91.5
Compound (2)	1×10^{-5}	5.2	194.1	0.858	85.8
	5×10^{-5}	5.1	197.0	0.860	86.0
	1×10^{-3}	4.5	223.6	0.877	87.7
	5×10^{-3}	4.2	243.8	0.887	88.7
Compound (3)	1×10^{-5}	7.3	138.4	0.801	80.1
	5×10^{-5}	5.8	174.9	0.843	84.3
	1×10^{-3}	5.1	200.2	0.863	86.3
	5×10^{-3}	3.9	258.8	0.887	88.7

3.4. Electrochemical Frequency Modulation (EFM)

EFM is a nondestructive corrosion measurement technique that can directly and quickly determine the corrosion current value without prior knowledge of Tafel slopes, and with only a small polarizing signal. These advantages of EFM technique make it an ideal candidate for online corrosion monitoring [42]. The great strength of the EFM is the causality factors which serve as an internal check on the validity of EFM measurement. The causality factors CF-2 and CF-3 are calculated from the frequency spectrum of the current responses. Figure (9) shows the frequency spectrum of the current response of pure carbon steel in 1 M HCl , contains not only the input frequencies, but also contains frequency components which are the sum, difference, and multiples of the two input frequencies. The EFM intermodulation spectrums of carbon steel in 1M HCl acid solution containing ($1x10^{-5}$ M and $5x10^{-3}$ M) of the studied inhibitors are shown in Figure (9). Similar results were recorded for the other concentrations of the investigated compounds (not shown). The experimental EFM data were treated using two different models: complete diffusion control of the cathodic reaction and the "activation" model. For the latter, a set of three non-linear equations had been solved, assuming that the corrosion potential does not change due to the polarization of the working electrode [43]. The larger peaks were used to calculate the corrosion current density (i_{corr}), the Tafel slopes (β_c and β_a) and the causality factors (CF-2 and CF-3).These electrochemical parameters were listed in Table (7). The data presented in Table (7) obviously show that, the addition of any one of tested compounds at a given concentration to the acidic solution decreases the corrosion current density, indicating that these compounds inhibit the corrosion of carbon steel in 1 M HCl through adsorption. The causality factors obtained under different experimental conditions are approximately equal to the theoretical values (2 and 3) indicating that the measured data

are verified and of good quality [44]. The inhibition efficiencies % IE $_{EFM}$ increase by increasing the studied inhibitor concentrations and was calculated from Eq.(13):

$$\% IE_{EFM} = [(1- i_{corr}/ i^{o}_{corr})] \times 100 \quad (13)$$

where i^{o}_{corr} and i_{corr} are corrosion current densities in the absence and presence of inhibitor, respectively. The inhibition sufficiency obtained from this method is in the order: compound (1) > compound (2) > compound (3)

Figure (9): EFM spectra carbon steel in 1M HCl in the absence and presence of different concentrations of compound (I) at 30°C

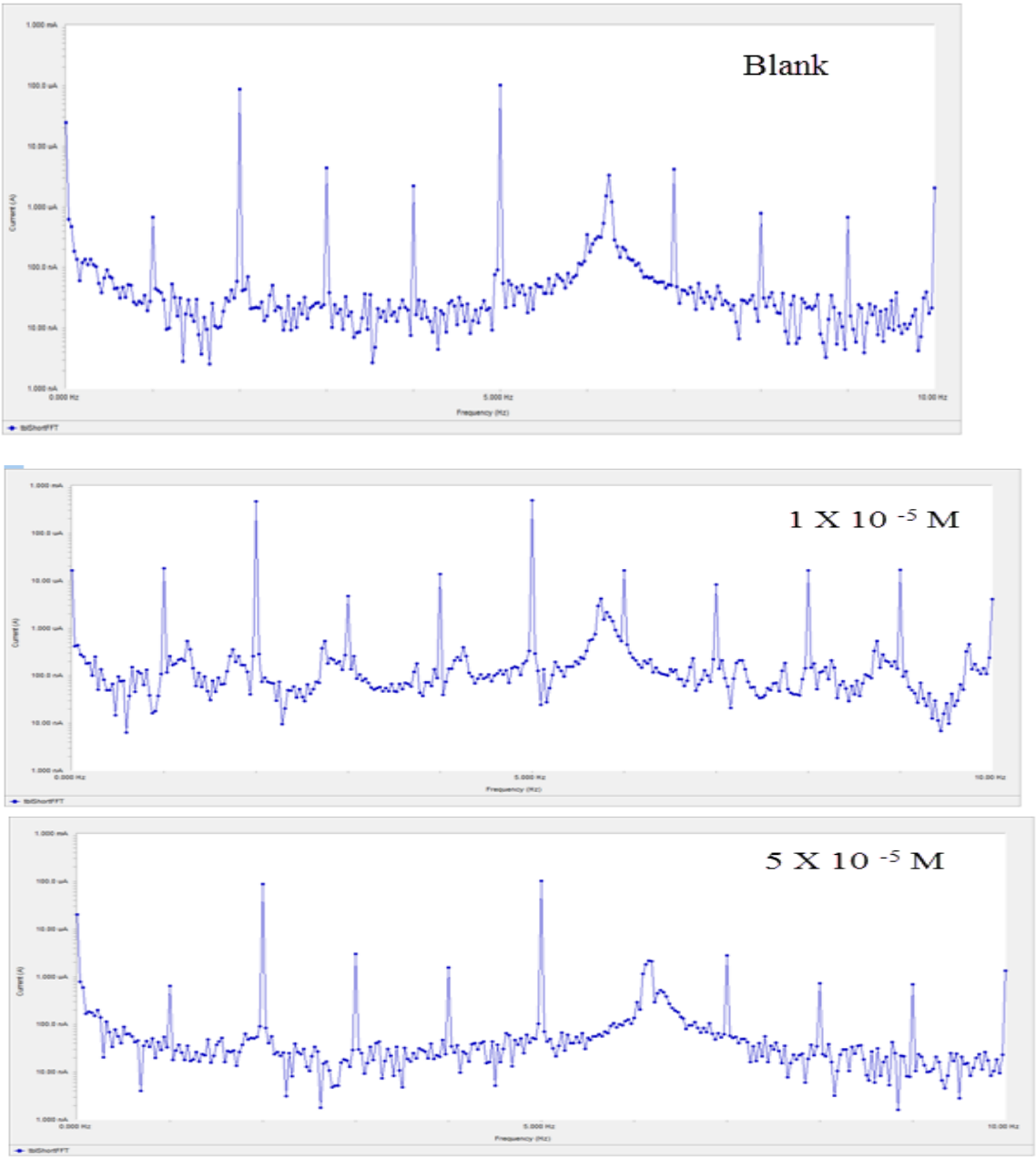

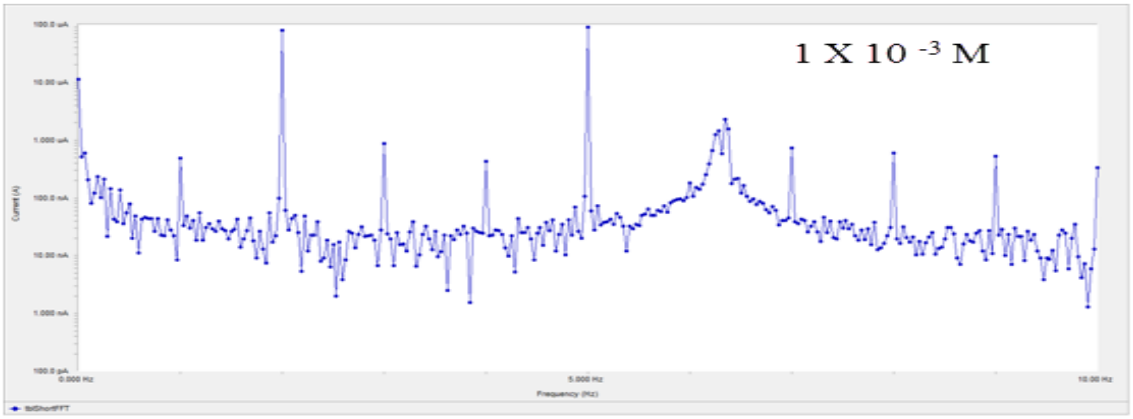

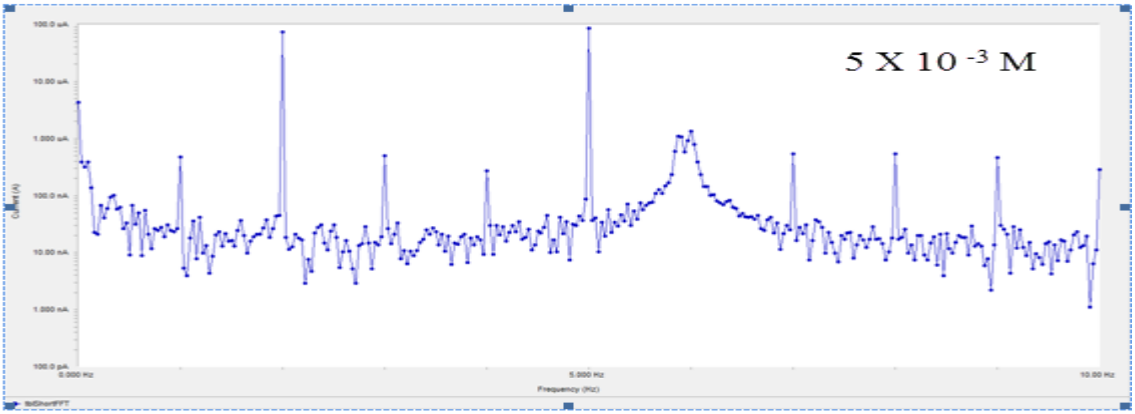

Table (7): Electrochemical kinetic parameters obtained from EFM technique for the corrosion of carbon steel in 1 M HCl at different concentrations of investigated inhibitors at 30°C

compounds	Conc, M	$i_{corr.}$ µA cm^{-2}	β_c , mV dec^{-1}	$\beta_{,a}$, mV dec^{-1}	CF(2)	CF(3)	θ	% IE
Blank	1 M HCl	458.5	60.1	63.3	1.15	3.04	----	----
Compound (1)	1×10^{-5}	375.8	117.5	174.5	2.01	3.40	0.615	61.5
	5×10^{-5}	272.2	122.9	160.2	2.04	2.90	0.675	67.5
	1×10^{-3}	201.0	139.5	151.7	2.10	3.00	0.677	67.7
	5×10^{-3}	195.4	143.6	152.4	1.20	2.90	0.694	69.4
Compound (2)	1×10^{-5}	205.2	127.3	190.2	2.02	3.70	0.552	55.2
	5×10^{-5}	202.7	120.0	136.7	2.05	2.50	0.558	55.8
	1×10^{-3}	189.9	131.7	141.8	2.10	2.40	0.586	58.6
	5×10^{-3}	180.4	140.4	149.4	1.90	2.70	0.606	60.6
Compound (3)	1×10^{-5}	375.8	117.5	174.5	2.01	3.40	0.615	61.5
	5×10^{-5}	272.2	122.9	160.2	2.04	2.90	0.675	67.5
	1×10^{-3}	201.0	139.5	151.7	2.10	3.00	0.677	67.7
	5×10^{-3}	195.4	143.6	152.4	1.20	2.90	0.694	69.4

3.5- Scanning Electron Microscopy (SEM) Studies

Figure (10) represents the micrography obtained for carbon steel samples in presence and in absence of 5x 10^{-3} M amide compounds after exposure for 3 days immersion. It is clear that carbon steel surfaces suffer from severe corrosion attack in the blank sample. It is important to stress out that when the compound is present in the solution, the morphology of carbon steel surfaces is quite different from the previous one, and the specimen surfaces were smoother. We noted the formation of a film which is distributed in a random way on the whole surface of the carbon steel. This may be interpreted as due to the adsorption of the amide compounds on the carbon steel surface incorporating into the passive film in order to block the active site present on the carbon steel surface. Or due to the involvement of inhibitor molecules in the interaction with the reaction sites of carbon steel surface, resulting in a decrease in the contact between carbon steel and the aggressive medium and sequentially exhibited excellent inhibition effect [45]

Figure (10): SEM micrographs for carbon steel in the absence and presence of 5x10^{-3} M of amide compounds

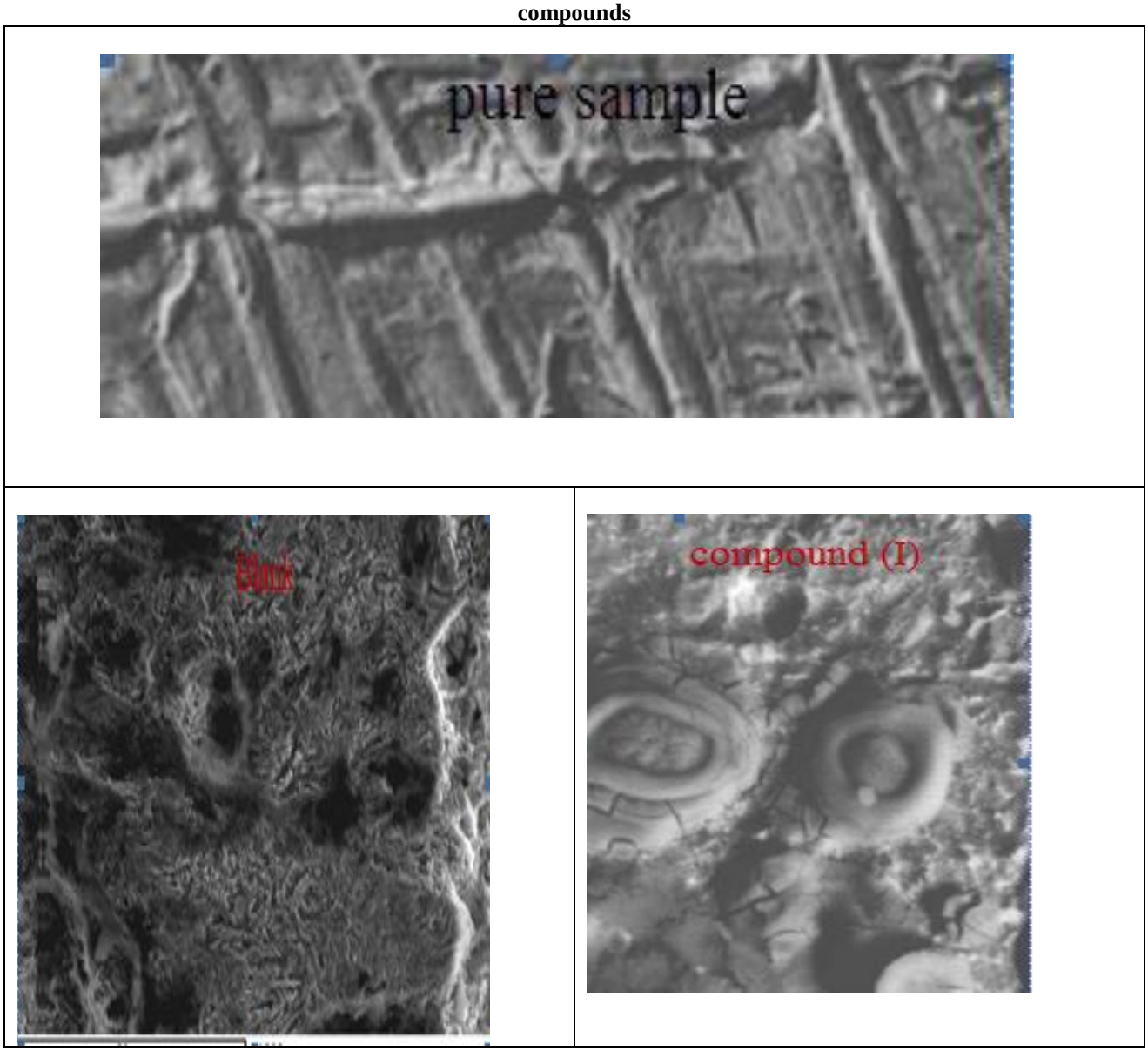

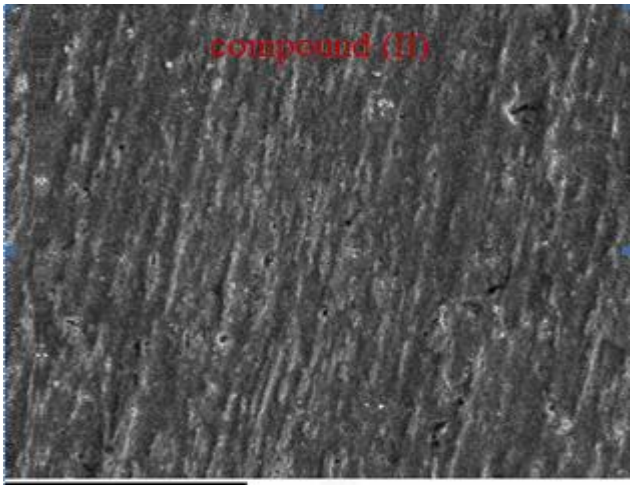

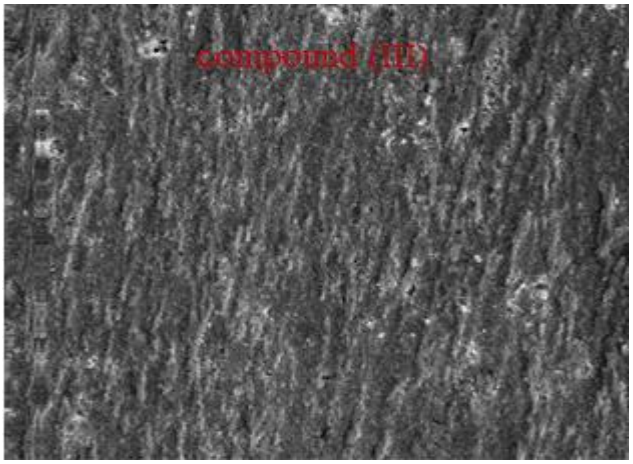

3.6. Energy Dispersion X-Ray Spectroscopy (EDX) Studies

The EDX spectra were used to determine the elements present on the surface of carbon steel and after 3 days of exposure in the uninhibited and inhibited 1 M HCl. Figure (11) shows the EDX analysis result on the composition of carbon steel only without the acid and inhibitor treatment. The EDX analysis indicates that only Fe and oxygen analysis of carbon steel in 1M HCl only and in the presence of $5x10^{-3}$ M of amide compounds. The spectra show additional lines, demonstrating the existence of C (owing to the carbon atoms of amide compounds). These data shows that the carbon and oxygen atoms covered the specimen surface. This layer is entirely owing to the inhibitor, because the carbon and O signals are absent on the specimen surface exposed to uninhibited HCl. It is seen that, in addition to Cr, C. and O were present in the spectra. A comparable elemental distribution is shown in Table (8).

Figure (11): EDX analysis on carbon steel in the presence and absence of amide compounds for 3 days immersion

Pure sample

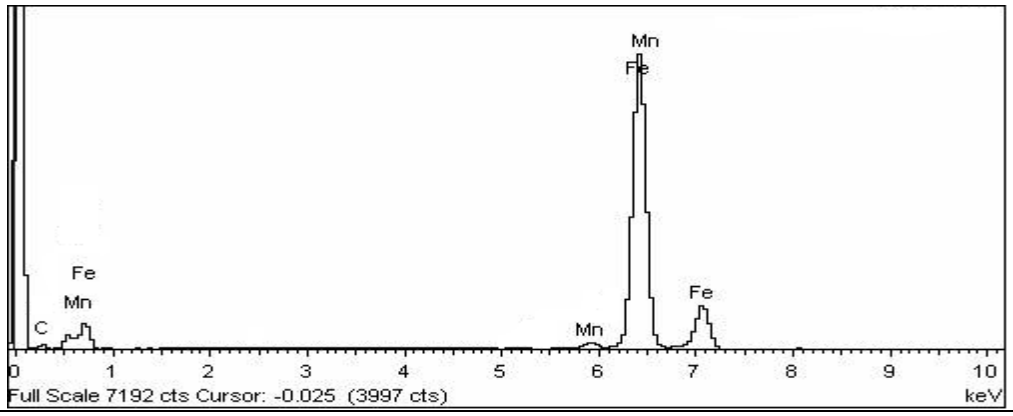

Blank

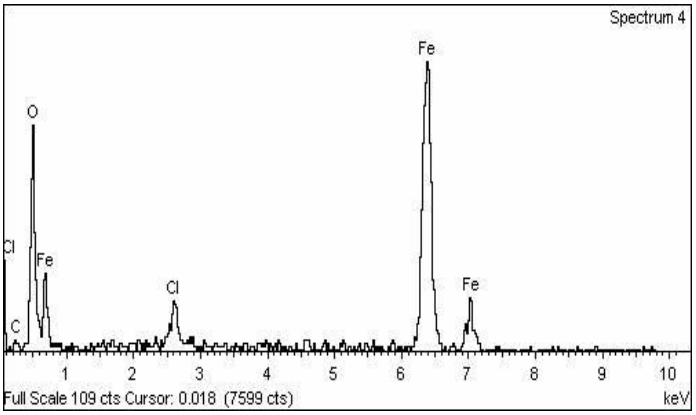

Compound(1)

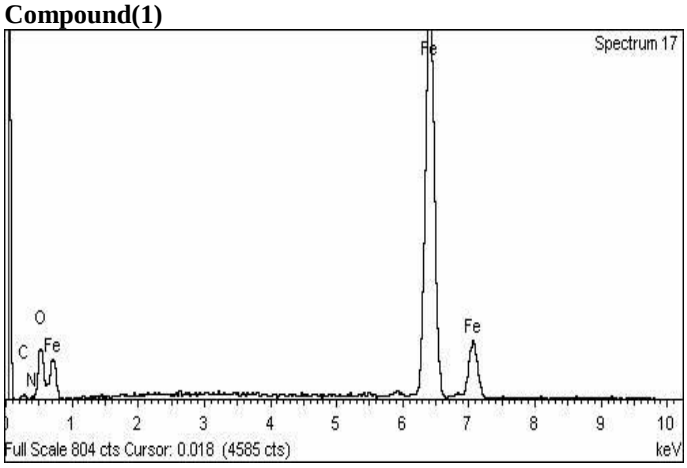

Compound(2)

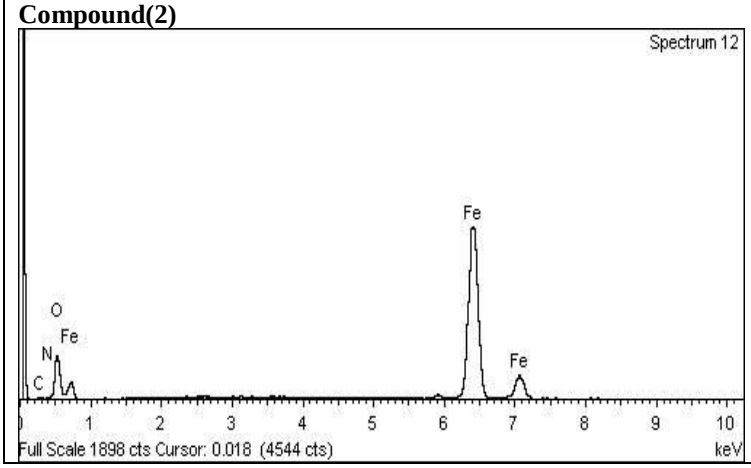

Compound(3)

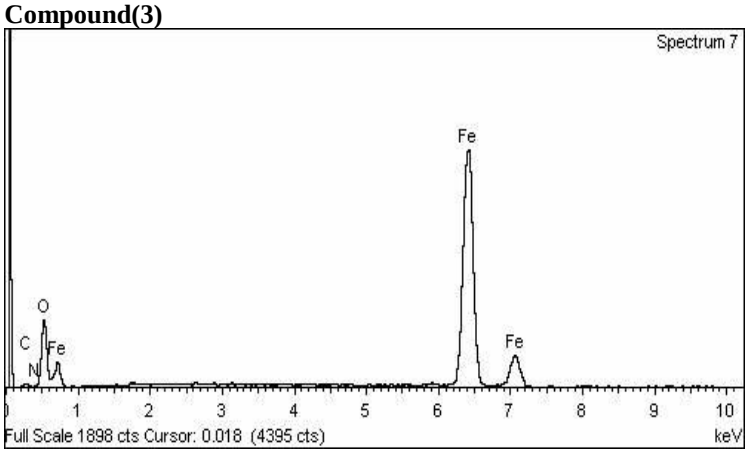

Table (8): Surface composition (weight %) of carbon steel after 3hrs of immersion in HCl without and with the optimum concentrations of the studied inhibitors

(Mass %)	Fe	C	O	N	Cr
Pure	79.09	2.09	--	--	0.82
Blank	55.49	2.81	31.61	7.86	--
Compound (1)	72.88	3.79	21.66	5.03	1.67
Compound (2)	62.37	3.40	32.53	5.74	2.30
Compound (3)	60.47	2.91	34.89	5.81	1.25

3.7. Quantum chemical calculations

Theoretical calculations were performed for only the neutral forms, in order to give further insight into the experimental results. Values of quantum chemical indices such as energies of LUMO and HOMO (E_{HOMO} and E_{LUMO}), the formation heat ΔH_f and energy gap ΔE, are calculated by semi-empirical PM3 methods has been given in Table (9). The reactive ability of the inhibitor is related to E_{HOMO}, E_{LUMO} [46]. Higher E_{HOMO} of the adsorbent leads to higher electron donating ability. Low E_{LUMO} indicates that the acceptor accepts electrons easily. The calculated quantum chemical indices (E_{HOMO}, E_{LUMO}, μ) of investigated compounds are shown in Table (9). The difference $\Delta E = E_{LUMO} - E_{HOMO}$ is the energy required to move an electron from HOMO to LUMO. Low ΔE facilities adsorption of the molecule and thus will cause higher inhibition efficiency. The bond gap energy ΔE increases from compound (1) to compound (3). This fact explains the decreasing inhibition efficiency in this order [compound (1) > compound (2) > compound (3)], as shown in Table (9) and Fig (12) show the optimized structures of the three investigated compounds. So, the calculated energy gaps show reasonably good correlation with the efficiency of corrosion inhibition. Table (9) also indicates that compound (1) possesses the lowest total energy that means that compound (1) adsorption occurs easily and is favored by the highest softness. The HOMO and LUMO electronic density distributions of these molecules were plotted in Figure (12). For the HOMO of the studied compounds that the benzene ring, N-atoms and O-atom have a large electron density. The data presented in Table (9) show that the calculated dipole moment decrease from [compound (1) > compound (2) > compound (3)]

Structure	HOMO	LUMO	Mulliken chargs
(1)	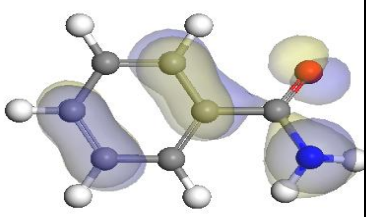	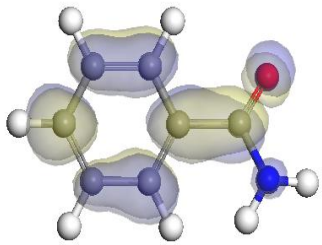	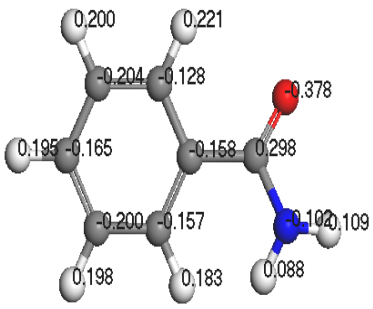
(2)	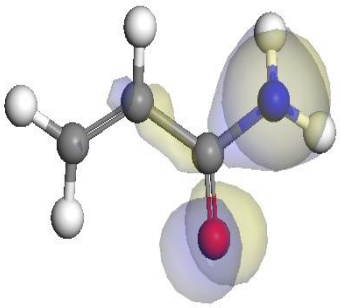	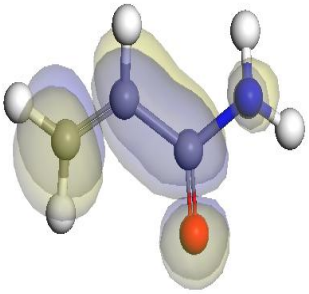	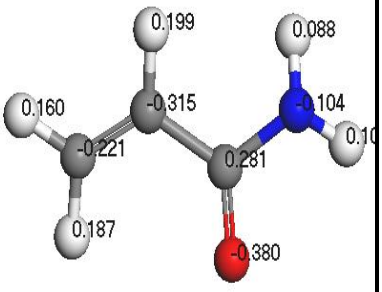

(3)	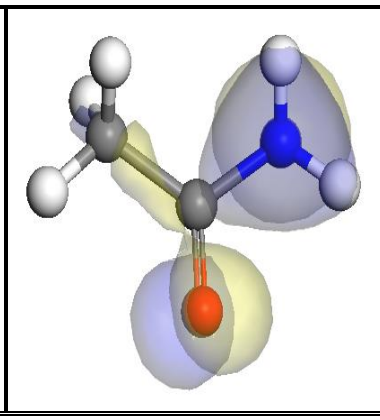	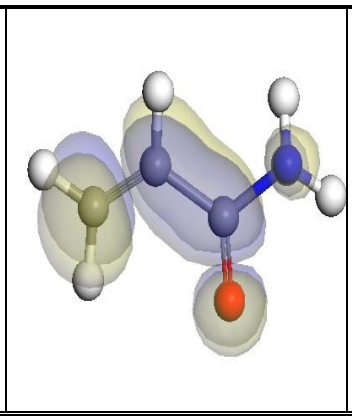	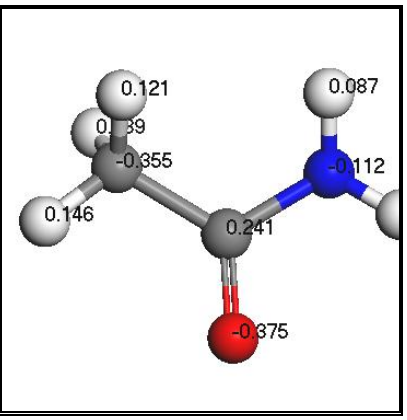

Figure (12): Molecular orbital plots and Mulliken charges of amide compounds

Table (9): The calculated quantum chemical properties for amide compounds

	Compound (1)	Compound (2)	Compound (3)
$-E_{HOMO}$ (eV)	10.042	10.024	10.88
$-E_{LUMO}$ (eV)	0.41	0.004	0.95
ΔE (eV)	9.632	10.02	9.930
Ƞ (eV)	4.816	5.01	4.965
σ (eV^{-1})	0.208	0.200	0.201
-Pi (eV)	5.226	5.014	5.915
χ (eV)	5.226	5.014	5.915
Dipole moment (Debye)	3.329	3.083	3.265
Area ($Å^2$)	146.876	102.996	88.539

4. Chemical Structure and Corrosion Inhibition

Inhibition efficiency of the carbon steel corrosion in 1 M HCl solution by some amide compounds using the above techniques was found to depend on the number of adsorption active sites in the molecule and their charge density, molecular size and stability of these derivatives in acidic solutions [47]. The order of increased inhibition efficiency for some amide compounds is: compound (1) > compound (2) > compound (3)

In acidic solutions, transition of metal/solution interface is attributed to the adsorption of the inhibitor molecules at the metal/solution interface, forming a protective film. The rate of adsorption is usually rapid and hence, the reactive metal surface is shielded from the acid solutions [48]. In fact, Adsorption process can occur through the replacement of solvent molecules from metal surface by ions and molecules accumulated in the vicinity of metal/solution interface. Ions can accumulate at the metal/solution interface in excess of those required to balance the charge on the metal at the operating potential. These ions replace solvent molecules from the metal surface and their centers reside at the inner Helmholtz plane. This phenomenon is termed specific adsorption, contact adsorption. The anions are adsorbed when the metal surface has an excess positive charge in an amount greater than that required to balance the charge corresponding to the applied potential. The exact nature of the interactions between a metal surface and an aromatic molecule depends on the relative coordinating strength towards the given metal of the particular groups present [49]. Generally, two modes of adsorption were considered. In one mode, the neutral molecules of amides can be adsorbed on the surface of carbon steel through the chemisorption mechanism, involving the displacement of water molecules from the carbon steel surface and the sharing electrons between the hetero-atoms and carbon steel. The inhibitor molecules can also adsorb on the carbon surface on the basis of donor–acceptor interactions between π-electrons of the Oxygen or nitrogen atoms and vacant d-orbitals of carbon steel surface. In another mode, since it is well known that the carbon steel surface bears positive charge in acidic solutions [50], so it is difficult for the protonated NH_2 group adsorbed through electrostatic interactions between the positively charged molecules and the negatively charged metal surface covered with Cl^- ions. As indicated from the different

methods: compound (1) has the highest percentage inhibition efficiency. This due to: (i) its larger molecular size (121.14) that may facilitate better surface coverage, (ii) its adsorption through two centers of adsorption (one oxygen and one nitrogen atoms) and iii) the presence of benzene ring . Compound (2) comes after compound (1) in inhibition efficiency; because it has lesser molecular size (71.08). But compound (3) has the lowest inhibition efficiency. Because it has the lowest molecular size (59.07)

5. Conclusions

The amide compounds show good corrosion inhibition property against carbon steel corrosion in 1M HCl solution. Inhibition efficiencies are related to concentration, temperature and chemical structure of the investigated compounds. Generally, inhibition efficiencies increase when concentration increases and temperature decreases. All investigated compounds affected both anodic and cathodic reactions, so they are classified as mixed type inhibitors. Adsorption of these derivatives on the carbon steel surface obeys Temkin adsorption isotherm. EIS measurements clarified that the corrosion process was mainly charge transfer controlled and no charge in the corrosion mechanism occurred due to the inhibitor addition to acidic solutions.

6. References

[1] M.A. Deyab, Corros. Sci. 49 (2007) 2315–2328.
[2] S.A. Abd El-Maksoud, A.S. Fouda, Mater. Chem. Phys. 93 (2005) 84–90.
[3] K.F. Khaled, Mater. Chem. Phys. 112 (2008) 290–300.
[4] E. Machnikova, K.H. Whitmire, N. Hackerman, Electrochim. Acta 53 (2008)6024–6032.
[5] H. Ashassi-Sorkhabi, M.R. Majidi, K. Seyyedi, Appl. Surf. Sci. 225 (2004)176–185.
[6] M.A. Migahed, I.F. Nassar, Electrochim. Acta 53 (2008) 2877–2882.
[7] G. Avci, Colloids Surf. A 317 (2008) 730–736.
[8] O. Benali, L. Larabi, M. Traisnel, L. Gengembra, Y. Harek, Appl. Surf. Sci. 253(2007) 6130–6139.
[9] F. Xu, J. Duan, Sh. Zhang, B. Hou, Mater. Lett. 62 (2008) 4072–4074.
[10] M.A. Khalifa, M. El-Batouti, F. Mahgoub, A. Bakr Aknish, Mater. Corros. 54 (2003) 251–258.
[11] Y. Abboud, A. Abourriche, T. Saffaj, M. Berrada, M. Charrouf, A. Bennamara, N. Al Himidi, H.Hannache, Mater. Chem. Phys. 105 (2007) 1–5.
[12] H. Wang, H. Fan, J. Zheng, Mater. Chem. Phys. 77 (2002) 655–661.
[13] K.F. Khaled, Electrochim. Acta 48 (2003) 2493–2503.
[14] A. Popova, M. Christov, S. Raicheva, E. Sokolova, Corros. Sci. 46 (2004)1333–1350.
[15] E.A. Noor, A.H. Al-Moubaraki, Mater. Chem. Phys. 110 (2008) 145–154.
[16] E. E. Ebenso : Mater. Chem. Phys. 71 (2002)62.
[17] A.S.Fouda, M.N.Moussa, F.I.Taha and A.I.Elnanaa, Corros.Sci., 26(9) (1986)719.
[18] M. Abdallah, E. A. Helal and A. S. Fouda : Corros. Sci., 48 (2006) 1639.
[19] E. E. Oguzie : Mater. Letters, 59 (2005) 1076.
[20] R. W. Bosch, J. Hubrecht, W. F. Bogaerts, B. C. Syrett, Corrosion 57 (2001) 60.
[21] S. S. Abdel–Rehim, K. F. Khaled, N. S. Abd–Elshafi, Electrochim. Acta51 (2006) 3269.
[22] A.Galal, N.F.Atta and M.H.Hassan, Mater.Chem.Phys. 89 (2005) 28-37.
[23] R. W. Bosch, J. Hubrecht, W. F. Bogaerts, B. C. Syrett, Corrosion 57 (2001) 60.
[24] S. S. Abdel–Rehim, K. F. Khaled, N. S. Abd–Elshafi, Electrochim. Acta 51 (2006)3269.
[25] E. Kus, F. Mansfeld, Corros. Sci. 48 (2006) 965.
[26] G. A. Caigman, S. K. Metcalf, E. M. Holt, J.Chem. Cryst. 30 (2000) 415.
[27] D.C. Silverman and J.E. Carrico, National Association of Corrosion Engineers, 44 (1988) 280.
[28] W.J.Lorenz and F.Mansfeld, Corros.Sci. 21 (1981) 647.
[29] F. L. Laque and H. R. Gapson; Corrosion resistance of metals and alloys; 2nd ed.,Reinhold publishing corporation, New York, (1963).
[30] A. S. Fouda, H. A. Mostafa, F. El-Taib and G. Y. El-Ewady, Corros. Sci., 47(2005)1988-2004.
[31] A.S.Fouda, A.A. Al-Sawary, F.Sh. Ahmed and H.M. El-Abbasy; Corros. Sci.; 51(2009)485.
[32] L. Riggs and R. M. Hurd; Corrosion; 23 (1967) 252.
[33] S. N. Banerjee," An introduction to Science of Corrosion and its Inhibition" Ox-anion Press, Pvt Ltd., New Delhi, (1985).
[34] T.P.Zhao and G.N.Mu, Corros.Sci., 41 (1999) 1937.
[35] M. K. Gomma and M. H. Wahdan; Mater. Chem. Phys. 39 (1995) 209.

[36] N. Cahskan and S. Bilgic, Appl. Suref. Sci., 153 (2000) 128.
[37] H. Fisher, Ann. Univ. Ferrera. Sez. 3 (Suppl. 3) (1960) 1.[36] E.Stupnisek-Lisac, A.Gazivoda and M.Madzarac, J.Electrochim.Acta, 47 (2002) 4189.
[38] G.N.Mu,X.H.L and Q.Quand J.Zhou, Corros.Sci., 48(2006)445
[39] I. Sekine, M. Sabongi, H. Hagiuda, T. Oshibe, M. Yuasa, T.Imahc, Y. Shibata, and T.Wake; J. Electrochem. Soc.; 139 (1992) 3167.
[40] L.Larabi, O.Benali, S.M.Mekelleche and Y.Harek, Appl.Surf.Sci., 253 (2006) 1371.
[41] M.Lagrenee, B.Mernari, B.Bouanis, M.Traisnel and F.Bentiss, Corros.Sci., 44 (2002) 573.
[42] G. A. Caigman, S. K. Metcalf, E. M. Holt, J.Chem. Cryst.30 (2000) 415.
[43] D.C. Silverman and J.E. Carrico, National Association of Corrosion Engineers, 44 (1988), 280.
[44] R.A., Prabhu, T.V., Venkatesha, A.V., Shanbhag, G.M., Kulkarni, R.G., Kalkhambkar,Corros.Sci., 50 (2008) 3356
[45] G., Moretti, G., Quartanone, A., Tassan, A., Zingales, , Wekst. Korros., 45(1994) 641
[46] C. Lee, W. Yang and R. G. Parr., Phys. Rev. B, 37 (1988) 785.
[47] E. Khamis, F. Bellucci, R.M. Latahision and E.Sh. El-Ashry, Corrosion 47 (9) (1991) 667.
[48] C. Y. Chao, L. F. Lin, and D. D. Macdonald,J. Electrochem. Soc., 128 (1981) 1187
[49] I. M. Ritchie, S. Bailey, and R. Woods, Adv. Colloid Interface Sci., 80 (1999) 183
[50] G. N. Mu, T. P. Zhao, M. Liu, and T. Gu, Corrosion